Heat Transfer in a Stud-to-Plate Laser Braze Considering Filler Metal Movement

A thermal computation model with the aid of a high-speed motion analyzer helps the development of a stainless steel to aluminum laser brazing process

BY J.-S. PARK AND S.-J. NA

ABSTRACT. A finite element model has been developed for the thermal analysis of a miniature stud-to-plate laser brazing process, and the transient temperature fields in the braze joint were analyzed by using an axisymmetric model. The finite element program ABAQUS, together with a few user subroutines, were employed to perform the numerical approximation. The joining materials used were AISI 304 stainless steel and Al 5052 aluminum, and the alloy 88Al-12Si for the braze filler metal. Nonlinear effect of temperature dependent thermal properties, latent heat and the convection and radiative heat losses were considered. The FE modeling was implemented with a non-coupled treatment of heat conduction and filler metal flow, while the model was based upon the real-time motion analysis of the brazing process. Definition of the FE solution domain and boundary conditions were crucial to achieve accuracy in predicting the transient thermal behavior, possible only with the aid of a high-speed camera. Numerical results of the temperature fields in the braze joint were obtained for typical process parameters. The predicted thermal histories show a fairly good agreement with the experimental ones that were determined by using the thermocouple and infrared temperature measurements.

Introduction

Aluminum-to-steel joints can be accomplished by fusion welding, brazing or solid phase joining methods. The choice is dependent upon the size of joining parts, the alloys used and the required joint properties. Riveting has also been widely utilized in the electronics industry to join small-size stainless steel studs onto aluminum plates; nevertheless a better technology has been sought to improve the productivity of the stud-to-plate joining process. Due to the inherent characteristics of laser beams, laser brazing is believed to be an alternative method for this dissimilar metal joint. The process is capable of producing a joint locally without heating the entire part or component to the flow temperature of the braze filler metal. A high degree of control is possible for the thermal energy by regulating the intensity, spot size, duration and precise location, which is particularly useful for the small or miniature part joining (Refs. 1–4).

The rate of heating and magnitude of thermal gradients are important factors in the quality of dissimilar metal joints. The effects of the process on the dimensional stability, residual stress and metallurgical structure of the braze joint must be considered. In the case of laser brazing for an aluminum-to-stainless steel joint, the temperature gradients produced in the joint are relatively large due to a great difference in the thermal properties and may cause the filler metal to flow in undesired directions; which may then impose difficulties in the control of the filler metal penetration into the braze gap. When the difference in melting points between the braze alloy and base metal is small, tight control of the brazing temperature is essential and the heating cycle must be short to minimize the thermal effect on the base metals. Thermal analysis of the braze joint is a prerequisite for designing the process parameters as well as the mechanical attributes of the joint, *i.e.*, the thermal distortion and residual stress. For predicting small-part joining processes, pure experimental approaches are sometimes not practical because of measurement difficulties, therefore, employing numerical approaches using computer simulation is beneficial.

In the past decades, numerous studies on laser material processing have been performed using analytical and numerical approaches. Most of the studies were rather process-oriented and concentrated on either laser cutting, welding or surface treatment — rarely on laser brazing (Refs. 5–11). We felt a study was needed to aid the development of the laser brazing process, including the process monitoring technologies (Ref. 12). In this paper, thermal behavior during the stud-to-plate laser brazing process has been analyzed using finite element (FE) modeling, with the FE model being based on experimental observation of the filler metal motion that occurs during brazing.

KEY WORDS

Numerical Analysis
Brazing/Soldering
Weld Process Simulation
LBW
Al-Alloys

Stud-to-Plate Laser Brazing Process

The schematic of the stud-to-plate laser braze with a cross section of workpieces is shown in Fig. 1. The workpieces consist of a 3-mm O.D. stainless-steel stud and a 1.2-mm thick aluminum-plate. Using a jig, an annular gap of

J.-S. PARK is a Supervisory Researcher, Mechanical Design Division, with Korea Power Engineering Company, Inc., and S.-J. NA is a Professor, Dept. of Mechanical Engineering, Korea Advanced Institute of Science and Technology, Yusong-Ku, Taejon, The Republic of Korea.

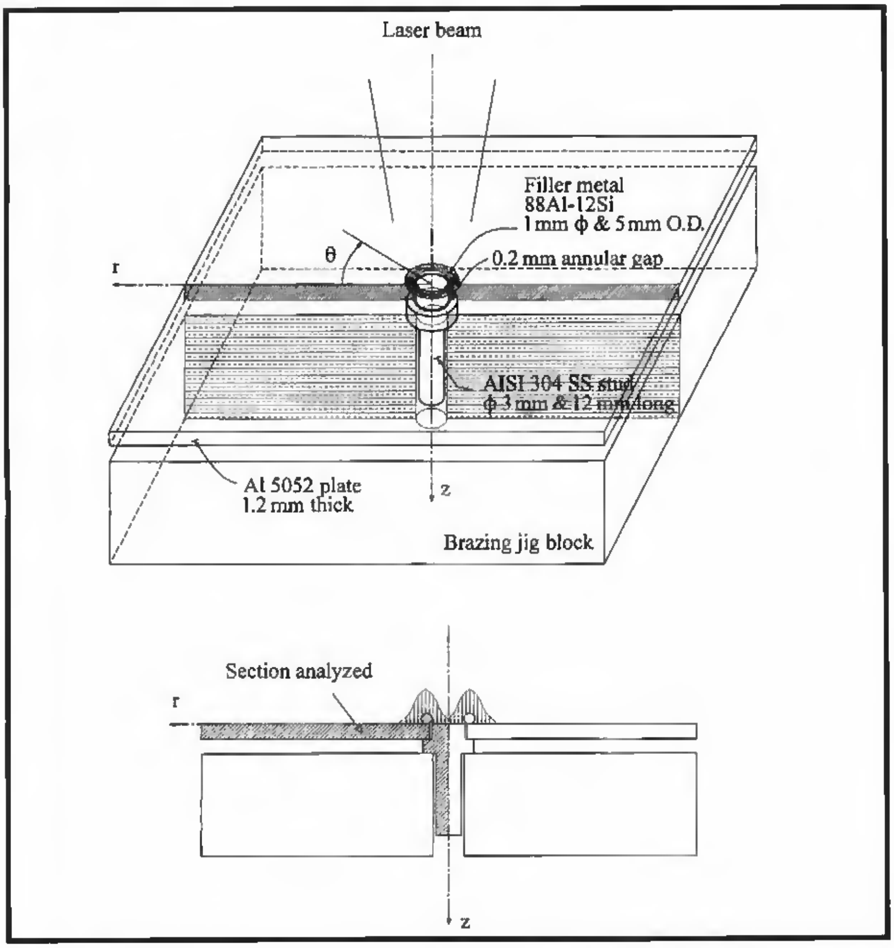

Fig. 1 — Schematic diagram of stud-to-plate laser braze (top) and a cross section of workpieces (bottom).

200 μm is provided initially between the brazing parts, and a ring-shaped filler metal is pre-placed on the plate around the periphery of the stud. Considering the shape of filler metal and the geometry of joint, a CW-CO_2 laser beam of a pseudo-TM_{01}* mode (the so-called doughnut mode) was chosen as the heat source. The joined materials were Al 5052 aluminum and AISI 304 stainless steel, and aluminum alloy 88Al-12Si was selected for the braze filler metal. The brazing is done in open air with the aid of a powder flux, and neither a pre-brazing nor a post-brazing heat cycle was attempted to control the thermal history of the joint. The studs to be joined function as guide posts or shafts for rollers, and the major quality factors are the perpendicularity of the stud with plate surface and the joint strength.

The CO_2 laser beam strikes the workpieces to heat locally in an area more than twice the diameter of the stud. The thermal diffusivity of aluminum is over ten times higher than that of stainless steel, thus requiring more energy input to the aluminum plate. The beam impingement area was about 7.5 mm diameter centered on the stud. This enabled both sides to be heated simultaneously for the filler metal to spread and penetrate into the braze gap. The braze flux melts within a few tenths of a second and covers the beam impingement area with a liquid film, and the filler metal being covered with the flux melts at the pre-placed location. The filler metal, once melted at the periphery of stud, instantly forms a small drop and moves towards the center of joint geometry, *i.e.*, the highest temperature region. The molten filler metal changes its free surface depending upon the wetting angles among the phases involved. Its wetting on the workpiece surface is retarded until the oxide film has been removed from the surface by reaction with the flux. After relocating on the top of the stud at the center, the filler metal starts to wet and spread over the workpieces as the heating cycle continues and, finally, is pulled into the annular gap by capillarity forces, leaving a round bead on the plate.

The thermal behavior of the filler metal during stud-to-plate laser brazing is dynamic in nature: the liquid drop motion, wetting and spreading. The filler metal movement is driven by the nonuniform temperature field, which is caused by the effect of localized heating of the laser beam and dissimilar metal workpieces. The motion of a liquid drop on the surface is a formidable fluid mechanics problem, the rigorous treatment of which is beyond the scope of this study. Further references on the subject can be found elsewhere (Refs. 13–15). When a temperature gradient is present on the surface of the liquid drop, an imbalance in the forces exists due to surface tension acting on the liquid-solid contact line of the drop. During stud-to-plate laser brazing, the filler metal drop moves a considerable distance on the workpiece surface before it wets and penetrates into the braze gap. This significantly affects the energy absorption of the incident beam, as well as the transient temperature field in the workpiece. Experimental observation of the filler metal during stud-to-plate laser brazing is described in more detail in the author's previous study (Ref. 16). As a result of preliminary tests performed on various joint geometries and filler metal types, the current joint configuration was chosen. Usually, the amount of filler metal in conventional brazing is controlled by the volume of the braze gap. For laser brazing, however, this is not true. Joint designs without the bead on the plate were not successful and all attempts to reduce the volume of filler metal also failed. When a smaller volume of filler metal is used, the gap penetration is not achieved and the filler metal solidifies in a drop form on the top of the stud, probably due to the effect of highly localized heating for dissimilar materials and the consequent high thermal gradient in the joint area.

Experiments

Experiments were designed to test the FE model as well as to validate the assumptions made for the thermal analysis of stud-to-plate braze. The experimental setup for CO_2 laser brazing is shown in Fig. 2. The brazing system consists of a power supply, laser delivery head, HeNe probe laser, CNC controller, X-Y table and computer. The laser is capable of maximum output power of 700 W and generates a continuous beam with a wavelength 10.6 μm in the TM_{00} mode. Through optical modulation using an axicon focusing, this Gaussian mode was transformed into a pseudo-TM_{01}* mode with a doughnut-shaped beam flux. The beam delivery head was fixed and the workpiece alignment was facilitated by an X-Y table and probe laser. A side blower using compressed air was also utilized to protect the optical parts from contamination. The surface of the stainless steel studs was prepared by pickling in a solution of 10% cold nitric acid and 0.25% hydrofluoric acid (room temperature) for 5 minutes, while the aluminum plate and filler metal were cleaned by vapor degreasing. After a series of tests on various combinations of the process parameters, the beam-on-time for brazing was determined to be 3 s at 550 W for a ring-shaped filler metal of 1 mm ϕ and 5 mm O.D. Temperature measurements of the filler metal under laser irradiation were made by using a noncontact infrared (IR) sensor. The IR sensor used was a PbSe photoconductive sensor with a peak wavelength of 3.8 μm, spectral response ranging from 1.5 to 4.8 μm and a cutoff wavelength of 4.8 μm. The IR sensor had an effective measurement spot of 4.0 mm diameter and had been calibrated by numerical simulation and thermocouple measurements (Ref. 12). The stud temperature was measured using a thermocouple attached below the bottom of the braze gap (z = 3.0 mm as noted in Fig. 7). The temperature measurements are plotted in Fig. 7 for comparison with the ones obtained by FE modeling.

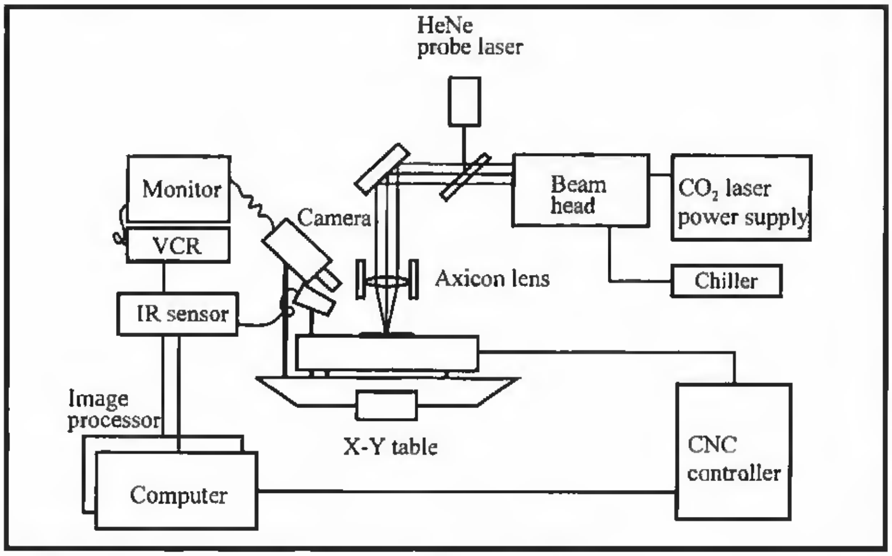

Fig. 2 — Experimental setup of stud-to-plate laser braze system.

Heat Transfer Analysis

Governing Equation and Boundary Conditions

We found that the heat transfer of our laser braze could be calculated by applying heat conduction theory, and the thermal and mechanical aspects of the problem could be decoupled without imposing a significant penalty on the calculation accuracy. The assumptions for this are that the dimensional changes during brazing are insignificant and that the mechanical work done is negligible compared to the thermal energy changes. Thermal energy changes resulting from the chemical reactions and evaporation of material occurring during brazing were also neglected. The energy equation of the problem without any internal heat generation is:

$$\rho C_p \frac{\partial T}{\partial t} = \underline{\nabla}\left(k \underline{\nabla} T\right) \tag{1}$$

Boundary conditions of the heat flux at surfaces were given by the Fourier equation:

$$\underline{q}'' = k \underline{\nabla} T \tag{2}$$

$$\iint_s k(T)\frac{\partial T}{\partial n} = -\iint_s A(T) I_0 dS$$
$$+\sigma \iint_s \varepsilon(T)\left(T^4 - T_0^4\right) dS + P_c$$

where:

$T(r, \theta, z, t)$ = temperature
P_c = heat loss by convection
n = surface normal
I_0 = power density of incident laser radiation
$k(T)$ = thermal conductivity
$\varepsilon(T)$ = hemispherical total emissivity
$A(T)$ = absorptivity at a laser wavelength

The heat flux q'' consists of the convective loss given by Newton's cooling law, the radiative loss given by the Stefan-Boltzmann equation and the specified heat flux at surfaces provided by the incident laser beam. Initial condition for the transient analysis is $T(r, \theta, z, t) = T_0(r, \theta, z)$ at time $t = 0$, where T_0 is the initial temperature.

Heat Input Model

Heat input by the incident laser beam can be modeled by applying the heat flux to the workpiece surface. The equation of heat flux for the pseudo-TM_{01}* mode can be formulated by introducing a radial shift r_{sh} into the TM_{00} mode energy distribution, as follows:

$$q''(r) = 3\frac{\alpha P}{\pi \bar{r}^{2}} \exp\left[-3\left(\frac{r - r_{sh}}{\bar{r} - r_{sh}}\right)^2\right] \tag{3}$$

In the above equation, r is the radial distance from the axis of impinging laser beam and $\bar{r}$ the characteristic radius (Gaussian beam radius) of the TM_{00} mode that is defined as the radial distance where the intensity of the beam falls to 5% of the maximum intensity. Total heat transferred to the substrate is $Q = \alpha P$, where α denotes the absorptivity of material and P the total incident of laser power. The value of r_{sh} varies with the defocusing of beams. By putting the total energy delivered in the TM_{01}* mode equal to the value in the TM_{00} mode, a multiplication factor of ratio to the right side of Eq. (3) is determined and this factor varies upon the shift distance r_{sh}. When defocused at a fixed beam diameter, if the shift distance r_{sh} is smaller than $\bar{r}/2$, then a nonzero center-fluxed distribution is obtained instead of the center-null one. A graphical representation of the heat flux from the pseudo-TM_{01}* mode for the values of r_{sh} = 1.45 mm and $\bar{r}$ = 3.75 mm is shown in Fig. 3.

Thermal Properties of Materials

As already noted, the materials used were Al 5052 aluminum plate and AISI type 304 stainless steel stud. Braze alloy 88Al-12Si (AWS BALSi-4; UNS A94047) was used as the filler metal, which is near the eutectic point of 12.7 wt-% silicon. The temperature-dependent thermal properties of materials were assumed isotropic and homogeneous. The latent heat of fusion used for Al 5052 was 408 kJ/kg, to be released or absorbed over the temperature range from T_S =

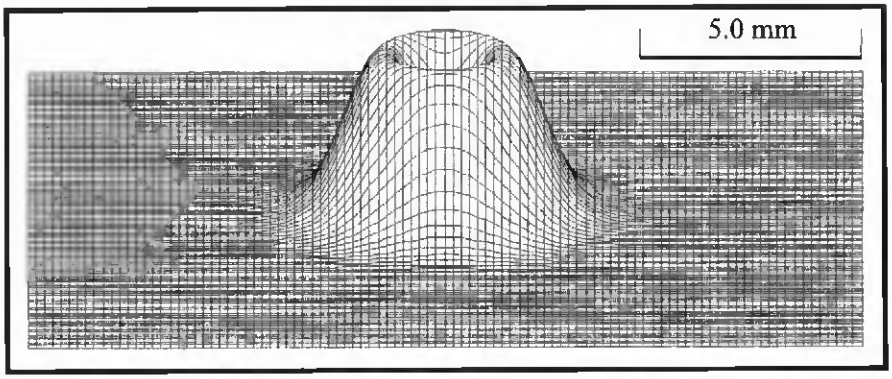

Fig. 3 — Contours of heat flux from an optically modulated TM_{01} mode laser beam (r_{sh} = 1.45 mm; r = 3.75 mm).*

607°C (1125°F) to T_L = 649°C (1200°F). Thermal properties of the braze alloy at high temperatures of interest were not available. The same values as those of Al 5052 were assumed except that the latent heat was applied over the temperature range from T_S = 577°C (1071°F) to T_L = 582°C (1080°F) by considering the contribution of each alloy constituent. Thermal properties of Al 5052 and 88Al-12Si alloy are comparable, except that they show a 12% difference in thermal conductivities at room temperature (Refs. 17–20). Consideration was given to simulating the stirring action inside molten filler metal, which increases by several times the rate of heat conduction into base metals. From the trial runs, an effective thermal conductivity k_{eff} — which was increased about two times the value of unstirred state — was used for the filler metal above its melting point.

Surface Heat Losses

During laser brazing, using the flux in the atmosphere, heat losses from the workpiece are through natural convection, radiation and evaporation of the molten metal or flux. Only convective and radiative heat losses were applied for this study. The convective heat loss is represented by Newton's cooling law $q'' = h\,(T-T_a)$, and the film coefficient used was h = 10 W/m² °K (Refs. 21–23). The radiative heat loss was calculated for the surfaces exposed to the atmosphere, using the Stefan Boltzmann equation $q'' = \bar{\varepsilon}\,\sigma\,(T^4 - T_a^4)$, for which the emissivity values of 0.25 for stainless steel and 0.09 for aluminum were assumed (Refs. 21, 24).

Absorptivity of Materials

The absorptivity values used for the thermal analysis of laser heating have a profound effect on the results. The absorptivity properties of metal surfaces for beam energy vary interactively upon the surface roughness, temperature and wavelength of the incident beam. Absorptivity of metal of infrared radiation increases drastically after its melting point is reached. Aluminum is a highly reflective material and its absorptivity of infrared energy at 10.6 µm (in the atmosphere) ranges from a value less than 10% at room temperature to between 40% and 50% at melting point, and goes as high as 90% at its vaporization point (Ref. 25). The same value of absorptivity as Al 5052 was used for the alloy 88Al-12Si. The absorptivity of type 304 stainless steel of CO_2 laser beam at 10.6 µm is less dependent upon the temperatures from room temperature to 1000°C (1832°F); it varies from 9% at room temperature to 12% at 1000°C depending on temperature and surface condition (Refs. 26–28). When surface oxide is present, the absorptivity of 304 stainless steel increases substantially, and it ranges from 12% at 800°C (1472°F) to approximately 40% at 1400°C (2552°F) (Ref. 27). It is noted that the absorptivity of stainless steels in the application of laser welding shows much higher values, up to 70% (Ref. 29). In the case of laser brazing studied here, the stainless steel stud does not melt and experiences an as-calculated maximum temperature of less than 900°C (1652°F). Therefore, the absorptivity of 304 stainless steel could be assumed to be constant at 10%, for simplicity.

When using a braze flux, the surfaces of the workpieces are covered with a thin film of molten flux, where chemical reactions to dissolve the metal oxides are occurring. The coverage of workpiece surfaces with the flux film was found to significantly enhance the absorption rate of beam energy. Based on the previous study of the laser heating for the materials used here, an effective absorptivity of 35% was applied for substrate materials when covered with molten flux (Ref. 12). The effect of evaporation from the flux has been reflected in the determination of the effective absorptivity, while energy change due to chemical reaction is negligible. So at a point when a surface becomes covered with molten flux, the constant absorptivity of 35% was used. Based on experimental observation, the selected locations of workpieces within an area of 6-mm radius from the center of joint geometry were assumed to be covered with liquid flux. They included the top surface of the stud, the aluminum plate around the braze gap and the filler metal. As observed, the powder flux melted and formed a liquid film within the beam-on-time of 0.1 s. for the given process condition. For convenience, the effective absorptivity was used from the beginning to the end of beam-on-time during the computation.

Solution Strategy and Analysis Method

The mathematical model of heat transfer in the stud-to-plate laser braze joint is one in which the transient temperature fields are strongly affected by the surface-tension-driven filler metal flow. The challenge is to treat the dynamic behavior of the filler metal without a decrease in accuracy and economy of the numerical analysis. Therefore, particular attention must be paid to simulate the filler metal movement.

Ideally, a fully coupled treatment of the heat conduction and filler metal flow would be employed to precisely predict the temperature field of the braze joint. This presumes a mathematical formulation of the filler metal flow, which includes the mechanics of a drop motion, wetting and spreading. The computation would be carried out for a single time step, and the element meshes for moving filler metal and the boundary conditions redefined before proceeding to the next time step of the analysis. However, the single time step analysis is impractical. An approximate solution in which a finite time step analysis assumed a discontinuous motion of the filler metal was adopted. In this study, finite element modeling was used to predict the transient temperature fields in the braze joint, not the filler metal motion. Definition of the solution domain and boundary conditions for the modeling was based on the results of experimental observations, and the motion of the filler metal was divided into a few stages. The free surface and thermal contact of the filler metal were assumed to be unaltered for a stage of computation model.

The transient temperature fields produced in laser brazing were analyzed by a two-dimensional FE model. Except for the treatment of molten filler metal, most of the FE modeling techniques developed to date in the area of welding mechanics can be utilized for the present study (Refs. 22–24, 30). The finite element program ABAQUS, together with a few user subroutines, was employed to conduct the numerical implementation. ABAQUS employs a front wave solver to solve the equation system by using Gaussian elimination, and the modified Newton method is used for the nonlinear heat transfer solution scheme. The iterative process is continued until the automatic convergence checking scheme has determined that the solution is accurate, where convergence criteria are applied on both the largest component of the residual flux vector and the size of the correction to the approximate solution. More information about the solution techniques is described in the ABAQUS theory manual (Ref. 31).

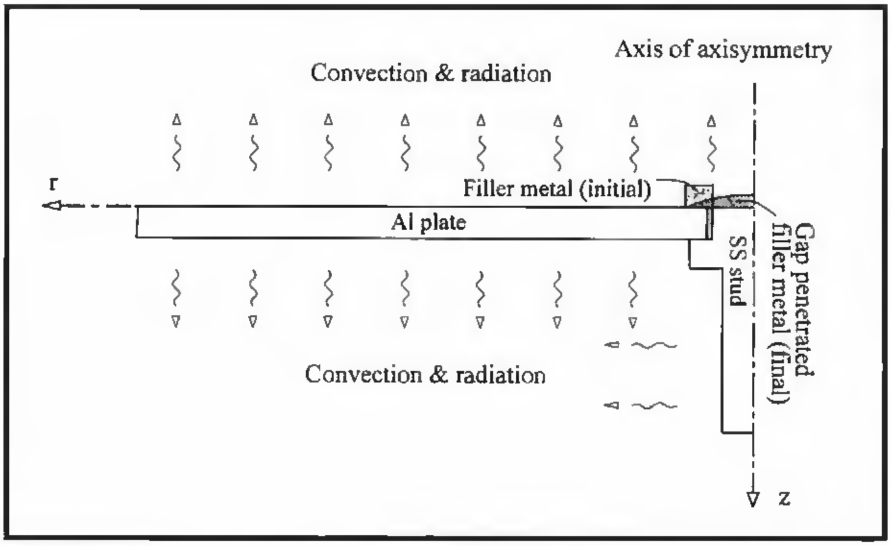

Fig. 4 — Thermal model for an axisymmetric FE analysis of stud-to-plate laser braze.

Finite Element Modeling

Axisymmetry of the braze joint geometry allows the temperature fields to be analyzed by a two-dimensional model. A thermal model for an axisymmetric FE analysis of stud-to-plate laser braze is shown in Fig. 4. For the discretization of the solution domain, linear elements that utilize a trapezoidal numerical integration scheme were used so that the discontinuous temperature gradient at the solid/liquid interface could be simulated smoothly and the adverse effects of the latent heat involved in the phase change could be minimized (Refs. 23, 31). Four-node isoparametric elements were employed for the whole domain except for the top surface of the stud, where three-node isoparametric elements were used to achieve the solution convergence.

When implementing the transient heat transfer analysis, an appropriate time-stepping scheme is required to ensure convergence and accuracy. The maximum temperature change (DELTMX) allowed in time increments controls the time integration accuracy. The automatic time stepping scheme restricts the time increment size so that DELTMX is not violated at any node (Ref. 31). A minimum time increment criterion based on the material's thermal properties and the characteristic length of element, was also applied for the transient solution of heat transfer. This criterion limited the size of element meshes for useful results. Trials were conducted on the fineness of element meshes, particularly for the area under the laser beams. The average linear size of elements used for the beam impingement area was 0.1 mm, while the total number of elements used was 860. The computation scheme using the ABAQUS program is shown in Fig. 5. In consideration of the fast heating and cooling during laser brazing, a relatively small time increment and less severe convergence criteria were used along with the automatic time integration scheme for a specified tolerance. The required time step depended upon the rate of temperature change between the time steps. It ranged from 3.56E-3 to 1.68E-2 s during the initial heating period up to 0.2 s and from 5.0E-3 to 4.3E-1s during the remainder of the braze cycle. The

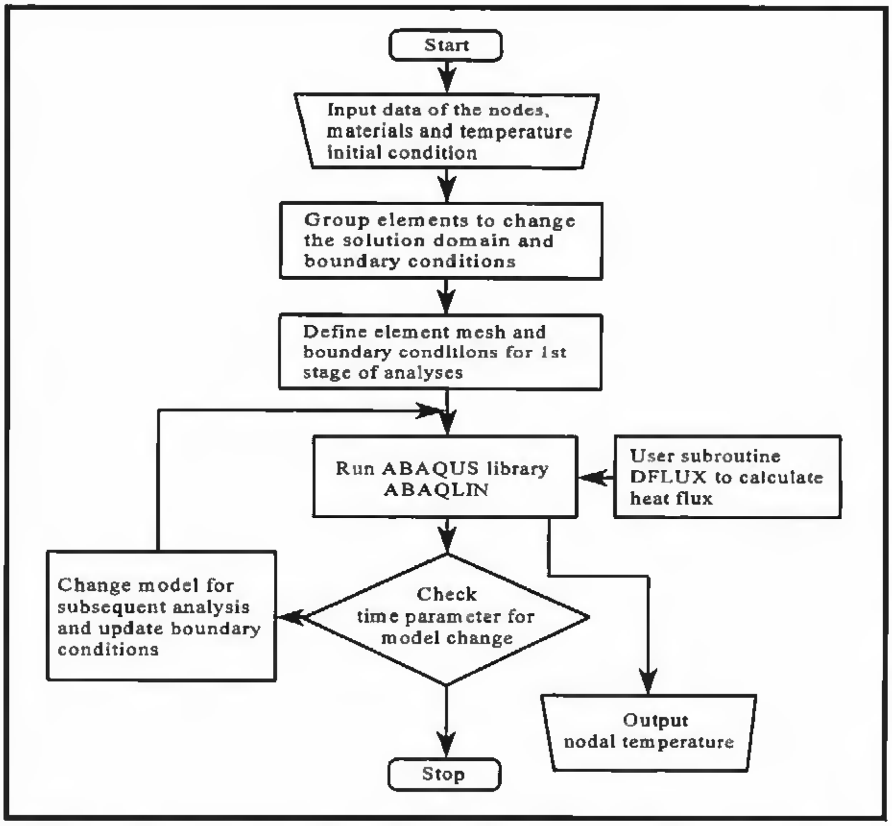

Fig. 5 — Flow chart for thermal analysis of stud-to-plate laser braze using ABAQUS program.

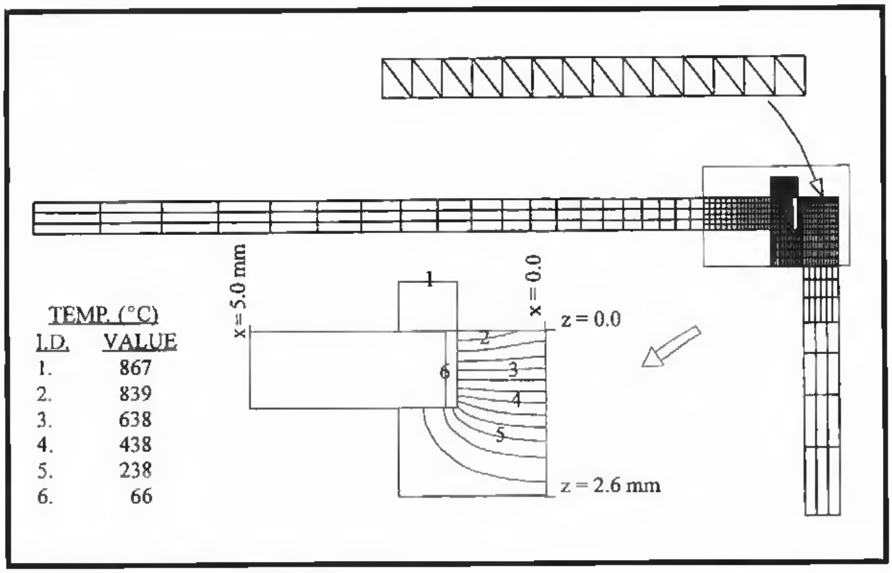

Fig. 6A — The first model for thermal analysis of stud-to-plate laser braze with filler metal pre-placed at initial location (at beam-on-time 0.2 s).

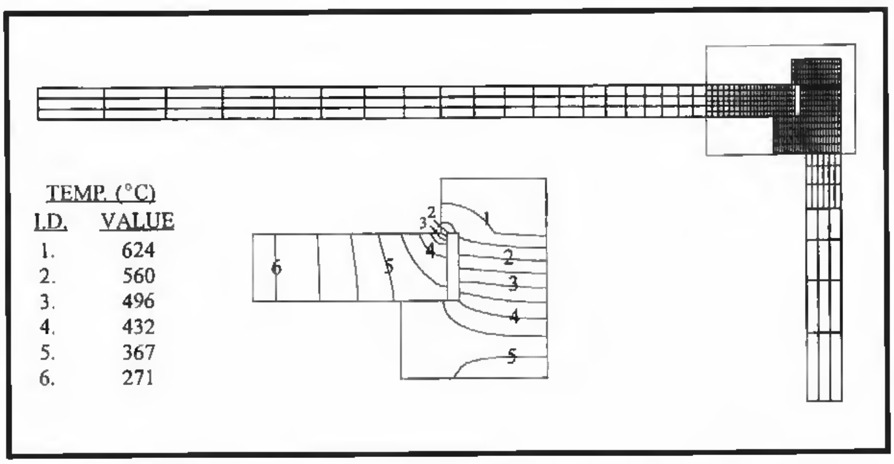

Fig. 6B — The second model for thermal analysis of stud-to-plate laser braze with filler metal relocated at center of joint (at beam-on-time 1.52 s).

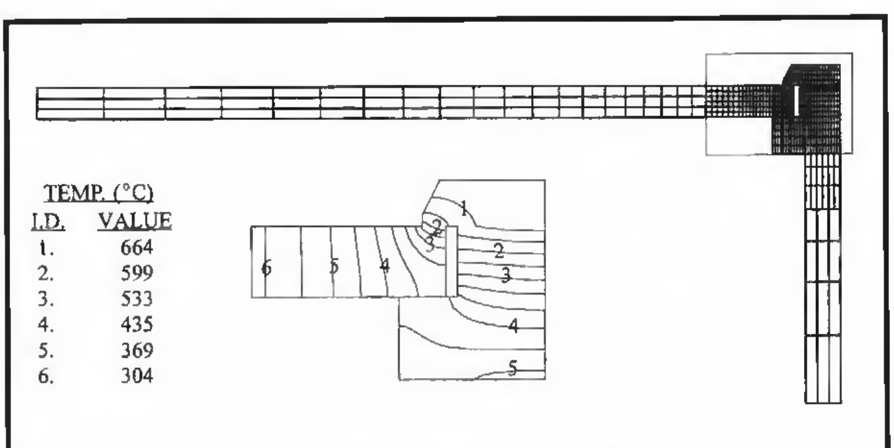

Fig. 6C — The third model for thermal analysis of stud-to-plate laser braze with partially spread filler metal at center of joint (at beam-on-time 1.68 s).

DELTMX applied was 200°C (392°F) for the initial heating and 100°C (212°F) for the remainder. The temperature tolerance (TEMTOL) used was 1% of DELTMX. The CPU time required to run for a complete braze cycle was 330 s on a CRAY supercomputer.

Six sets of the solution domain were defined for the transient thermal analysis of the laser brazing process, which were based on the results of experimental observation of the filler metal behavior for the given process condition. It was assumed for the definition of the FE solution domains that the free surface of the filler metal remained fixed for a period of time and then changed instantly to the next one for another stage of computation. The FE models used are shown in Figs. 6A–6F, along with the calculated temperature contours in the joint area, which also show the pre-placed, relocated at the center, partially and fully spread and the gap-penetrated filler metal, respectively. For each computation stage, the Model Change option as provided by ABAQUS was utilized. An intermediate stage to apply the boundary conditions was required before proceeding with the main computation for the specified boundary condition. During the Model Change, the temperature fields for the filler metal remained unaffected, except for temperatures at the interface nodes, where the average values were taken with the matching base metal nodes. The nodal temperatures of the base metals uncovered by the movement of the filler metal were kept constant from the previous step's values. Throughout the beam-on-time the energy input from the incident beam was applied as a time constant heat flux in the TM_{01}* mode, and the convective and radiative heat losses were considered for all surfaces except for the area covered with the braze flux. The thermal behavior of the braze flux was not modeled for simulation, except that its effect on the absorptivity and thermal insulation for the workpieces was considered.

The first solution model of Fig. 6A corresponds to the time period of initial heating, where the filler metal heats up and melts at the pre-placed location on the plate. For convenience, the filler metal was modeled using an equivalent rectangular cross section. The interface between the bottom of the filler metal and the top of the plate was assumed to be adiabatic, because thermal contact between the parts is inadequate until the filler metal melts completely. This assumption sacrifices the solution accuracy for the time period from the filler metal's melt-down to its relocation at the center. The time period allowed for the first model was up to the point of complete melting of the filler metal; then the model was changed to the second one, defined for the relocated filler metal. The second model, Fig. 6B, depicts the filler metal drop that has moved to the center of the joint, where it wets the top surface of the stud and the edge of the aluminum plate near the gap. Thermal contact at the surfaces wetted with the molten filler metal was assumed to be perfect. The second model was allowed to last until the surface temperature of the plate reached the flow point of the filler metal; it was followed by the models where the filler metal spread in the radial direction. The third and fourth models of Figs. 6C and 6D describe filler metal that has been partially (C) and fully (D) spread over the surface of the aluminum plate, respectively. The third model was introduced when the filler metal in the second model heated the plate sufficiently for the filler metal to spread to the size of 4.2 mm diameter (at beam-on-time 1.68 s), and after a further period of time (at beam-on-time 1.91 s), the model was changed to the fourth one for the fully spread filler metal at 5.0 mm diameter, as observed by experiments. That is, when the nodal temperature at the next discrete filler spread location reached the flow point of filler metal, the filler metal was allowed to spread (*i.e.*, the model was changed). As the heating cycle continued, the braze gap boundaries heated up sufficiently for the filler metal to penetrate. The fifth and sixth models of Figs. 6E and 6F depict the filler metal penetrating partially and completely into the braze gap, respectively. The gap penetration distance for the filler metal was limited to the extent where the nodal temperature exceeded the flow point of the filler metal. The time period permitted in each of these models was determined during the computation by examining the temperature histories at the gap boundaries. Following the sixth model, the beam was shut off and the workpiece began to cool.

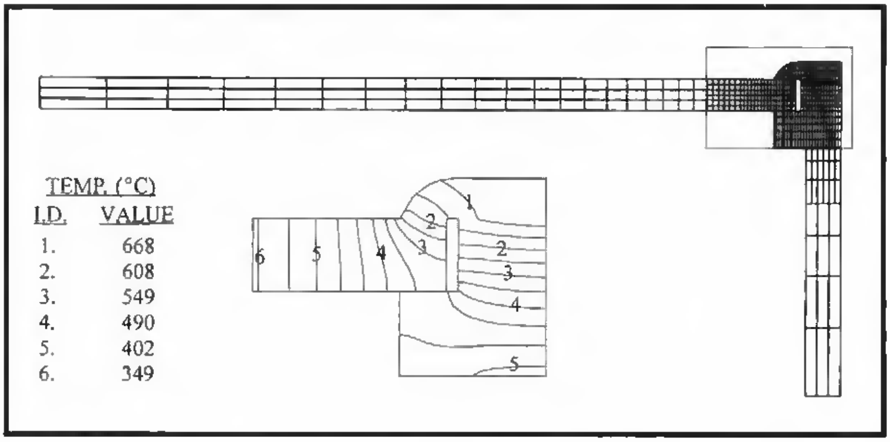

Fig. 6D — The fourth model for thermal analysis of stud-to-plate laser braze with fully spread filler metal (at beam-on-time 1.91 s).

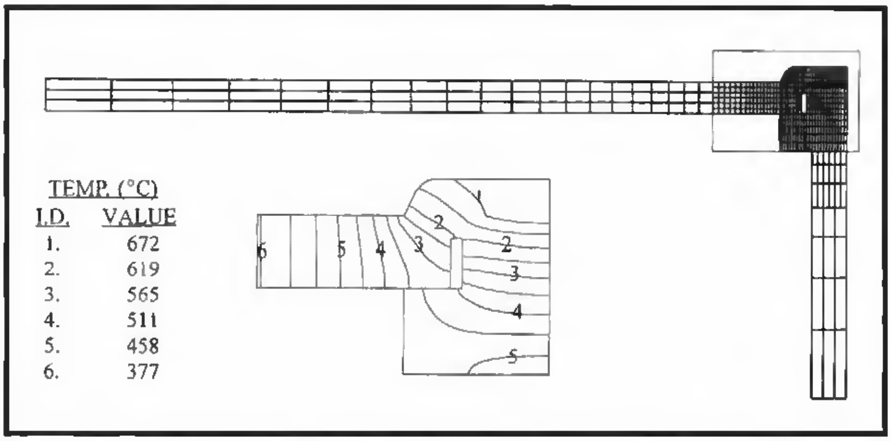

Fig. 6E — The fifth model for thermal analysis of stud-to-plate laser braze with partially gap-penetrated filler metal (at beam-on-time 2.37 s).

Results and Discussion

The calculated temperature contours in the joint area are also shown in Figs. 6A–6F. The contours were obtained for the beam-on-time of 3.0 s at the beam power of 550 W, and they cover those of the initial heating, relocation and wetting, spreading and gap penetration of the filler metal, respectively. In Fig. 7, a comparison was made between the predicted temperature histories and the ones determined by infrared and thermocouple measurements.

Figure 6A shows the isotherms in the joint area at the beam-on-time of 0.2 s, where the top of filler metal has been heated up to 867°C (1593°F) while the bottom surface is insulated from the plate. Because of the high thermal diffusivity, the calculated maximum temperature in the aluminum plate was only 66°C (151°F) near the braze gap, while the top of the stainless steel stud was heated up to 840°C (1544°F) on an average and the temperature gradient produced in the stud was as high as 293.6°C (560°F)/mm. The thermal diffusivity of the stainless steel stud is less than one-tenth of the aluminum plate. Figure 6B depicts the isotherms for the relocated filler metal at the beam-on-time of 1.52 s. The filler metal, once relocated and wetted on the workpieces, cooled rapidly to 610°C (1130°F), and the aluminum plate had been heated locally to the extent that the filler metal had spread on it. One notices during the second stage, the aluminum plate is apparently heated more by conduction from the filler metal than by direct absorption of the incident laser beam. The isotherms for the partially and fully spread filler metals at the beam-on-time of 1.68 s and 1.91 s, are depicted in Figs. 6C and 6D, respectively. Throughout the third and fourth stage, the filler metal undergoes a small temperature variation in the range of 664–668°C (1227–1234°F), by means of a slight thermal imbalance between influx from incident beams and efflux by conduction into the base metals. Without careful balance, the filler metal will melt the aluminum plate or cool so that no further spreading or gap penetration can occur. The interior of the workpieces are heated only through heat conduction from the top, and it takes a while for the heat at the top to diffuse to the bottom. At the beam-on-time of 1.91 s in Fig. 6D, the gap boundaries on both sides were heated sufficiently (600°C/ 1112°F) so that the filler metal could partially penetrate into the braze gap, but the temperature gradi-

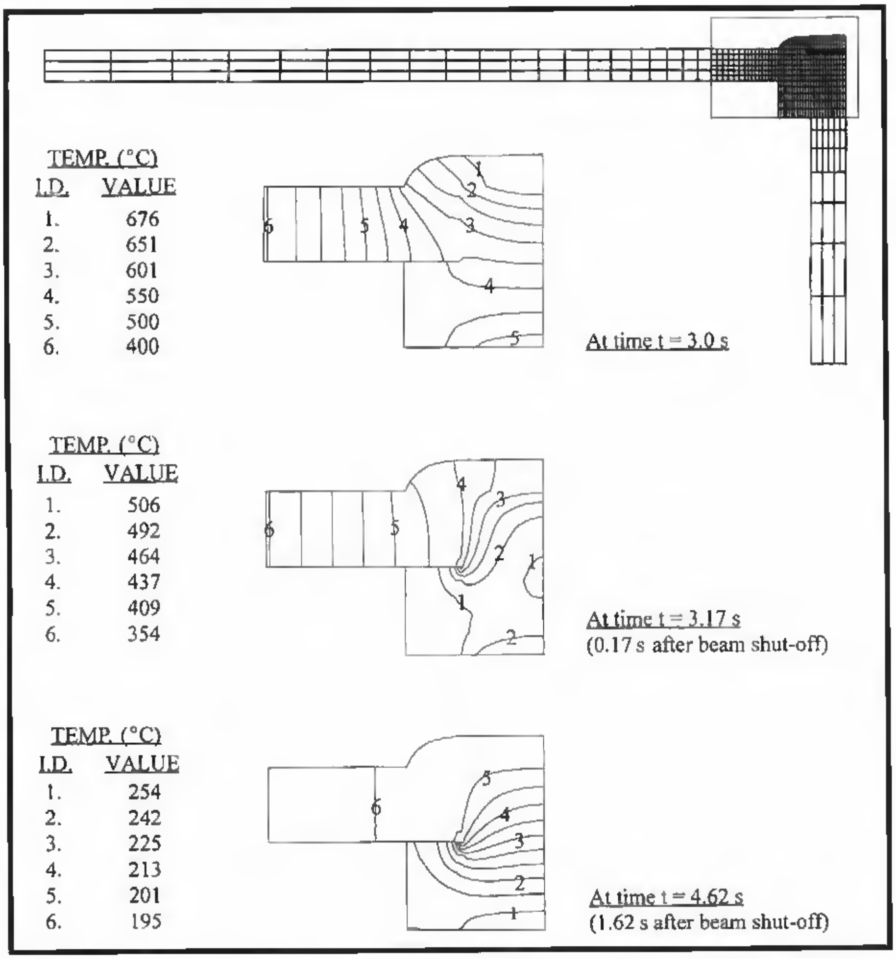

Fig. 6F — The sixth model for thermal analysis of stud-to-plate laser braze with completely gap-penetrated filler metal.

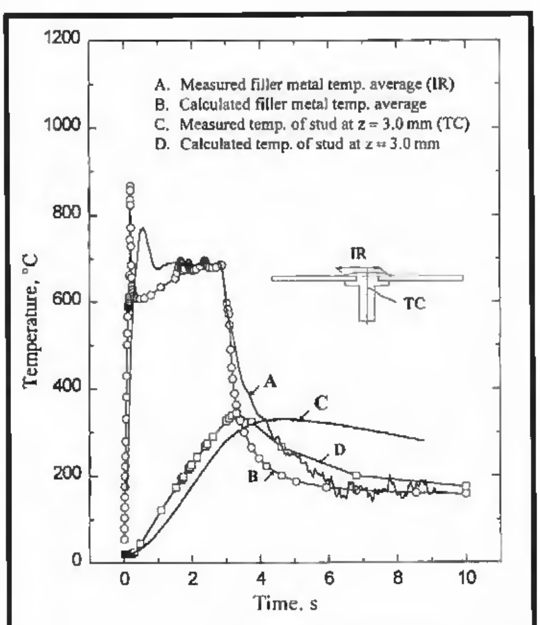

Fig. 7 — Predicted temperature histories of stud-plate laser braze workpieces and comparison with measurements by infrared and thermocouple.

ent along the gap boundaries was still high. Figures 6E and 6F show the isothermal contours for the partially and completely gap-penetrated filler metals, respectively. Based on the previous temperature fields developed around the gap boundaries, it was considered that the filler metal had penetrated into the gap to one-third of the gap length (1.2 mm) at the beam-on-time of 1.91 s and then to the bottom at the beam-on-time of 2.37 s. With the filler metal having penetrated into the gap, the temperature gradients around the joint area are substantially reduced by the metallurgical connection between the parts. Figure 6F depicts the temperature contours at the end of heating cycle (*i.e.*, beam-on-time 3.0 s), and at 0.17 s and 1.62 s after the beam shut off. As the beam was shut off, the joint began to cool rapidly and heat flow occurred from the stainless steel stud to the aluminum plate. It is noted that until the filler metal penetrated into the braze gap, the base materials had been heated mainly by the molten filler metal, and the temperature in the aluminum plate had remained below its melting point.

Figure 7 plots the temperature histories of the braze joint. The computed results of the filler metal temperature for the initial step predict a higher peak value and much faster heat-up than the infrared measurement showed. The measured and calculated heating rates of the top surface of the filler metal were found to be approximately 4330°C/s and 1288°C/s (7826°F/s and 2350°F/s), respectively, while the highest temperatures reached on the top surface at the end of the initial heating period were 867°C (1593°F) calculated and 773°C (1453°F) measured, respectively. This is probably due to the boundary conditions used in the model, in which the bottom of the filler metal is insulated from the plate. Another source of error was the assumption that the powder flux melts at the start of the beam-on-time and instantly increases the beam absorption to 35% for the workpieces. During the second computation stage for the relocated filler metal, the predicted temperatures differed substantially from the measurements, suggesting a much faster cool down and lower peak value. This discrepancy is probably due to the inherent deficiency of the model in which dynamics of molten filler metal have not been simulated rigorously. In reality, the molten filler metal moves around and is finally relocated at the center of joint within a few tenths of a second, but not instantly. Another probable source of error is the thermal behavior of the braze flux, which was not rigorously considered in the model. The major effect of existence of liquid flux covering the workpieces is to increase the laser absorption and to insulate the workpiece surfaces from heat losses to atmosphere. For the period after the filler metal has relocated to the center, the prediction is in fairly good agreement with the measurement. From the brazing process simulation point of view, the solution accuracy is less important during the initial transient period up to the filler metal's relocation, hut more critical for the remainder of the braze cycle, including the filler metal spreading and penetrating into the gap. After the beam was shut off, the braze filler metal underwent rapid cooling at a maximum rate of 460°C/s (B60°F). The model predicts a higher cooling rate (1323°C/s to 300°C) (2413°F/s to 572°F) than the measurement showed, which likely is due to the thermal blanketing effect of the solidified braze flux, as well as inherent errors in the IR measurement at low temperatures. The calculated results of the temperature history in the stud (at z = 3.0 mm) predict a slightly higher peak value with a time offset, *i.e.*, 342°C (648°F) at t = 3.304 s, and a faster cooling rate than the thermocouple measurements show. This discrepancy is likely due to the assumptions and boundary conditions used in the model. On the whole, the simulated temperature histories resulted in a fairly good qualitative agreement with the measurements.

Conclusions

From the results of the FE modeling for the heat transfer analysis of the stud-to-plate laser brazing and experiments, it has been revealed that a correct definition of the solution domain and boundary conditions is crucial to achieve an accuracy of the non-coupled numerical approximation. A simple assumption that, once melted, the filler metal instantly penetrates the braze gap and may cause significant error in predicting the transient temperature fields. The filler metal movement occurring in the stud-to-plate laser braze is due to the highly localized heating and the resulting non-uniform thermal fields on the workpiece, strongly affecting the transient temperature field of the dissimilar metal joint. With the aid of a real time motion analysis, motion of the filler metal was considered in defining the FE solution domain and boundary conditions. Without using a fully coupled analysis of the heat conduction and filler metal flow, the FE model presented is capable of predicting the temperature history of stud-to-plate laser braze with reasonable qualitative accuracy, and the results can be used further for qualitatively analyzing the distortion or residual stresses of the joint. The joining of a stainless steel stud to an aluminum plate by laser brazing is a new technology, which is still under development. For a laser brazing performed in a few seconds by localized surface heating, control of thermal conditions in the workpiece is critical, even more so for dissimilar metal braze joint. In future work, the FE model used here will be refined to more accurately simulate the filler metal behavior and developed further to fulfill a coupled solution of the heat conduction and filler metal flow problem.

References

1. Witherell, C. E., and Ramos, T. J. 1980. Laser brazing. *Welding Journal* 59(10): 267-s to 277-s.

2. *Brazing Manual*, 3rd ed., revised. 1976. American Welding Society, Miami, Fl.

3. Jones, T. A., and Albright, C. E. 1984. Laser beam brazing of small diameter copper wires to laminated copper circuit boards. *Welding Journal* 63(12): 34–47.

4. Witherell, C. E. 1981. Laser microbrazing to join small parts. *Laser Focuses*: 73–80.

5. Arata, Y., and Miyamoto, I. 1972. Some fundamental properties of high power laser beam as a heat source (Reports 1, 2 and 3). *Trans. Japan Welding Society* 3(1): 143–180.

6. Sparks, M. 1976. Theory of laser heating of solids: Metals. *J. Applied Physics* 47(3): 837 to 849.

7. Cline, H. E., and Anthony, T. R. 1977. Heat treating and melting material with a scanning laser or electron beam. *J. Applied Physics* 48(9): 3895–3900.

8. Lax, M. 1977. Temperature rise induced by a laser beam. *J. Applied Physics* 48(9): 3919–3924.

9. Moody, J. E., and Hendel, R. H. 1982. Temperature profiles induced by a scanning CW laser beam. *J. Applied Physics* 53(6): 4364–4371.

10. Mazumder, J., and Steen, W. M. 1980. Heat transfer model for CW laser material processing. *J. Applied Physics* 51(2): 941–947.

11. Yang, Y.-S. 1991. *A Study on the Residual Stress in Thermal Processing by the Arc and Laser Beam*. Ph.D. diss., Advanced Institute of Science and Technology, Seoul, Korea.

12. Jeon, M.-K. 1995. *A Study on Analysis of Heat Flow and Development of Temperature Measuring System in Laser Brazing*. Master's thesis. Advanced Institute of Science and Technology, Taejon, Korea.

13. Milner, D. R. 1958. A survey of the scientific principles related to wetting and spreading. *British Welding Journal* 5: 90–105.

14. Ehrhard, P., and Davis, S. H. 1991. Non-isothermal spreading of liquid drops on horizontal plates. *J. Fluid Mech.* 229: 365–388.

15. Ambrose, J. C., Nicholas, M. G., and Stoneham, A. M. 1992. Dynamics of braze spreading. *Acta metall. Mater.* 40(10): 2483–2488.

16. Park, J.-S., Chang, W.-S., Chang, H.-J., and Na, S.-J. 1996. A three-dimensional finite element analysis of thermal behavior in stud-to-plate laser brazing. *Proc. 6th. Int. Conf. in Computer Technology in Welding*. ed. W. Lucas, Paper No. 52. The Welding Institute, Abington, Cambridge, UK.

17. Rybicki, E. F., Schmueser, D. W., Stonesifer, R. W., Groom, J. J., and Mishlerl, H. W. 1978. A finite element model for residual stresses and deflections in girth-butt welded pipe. *Trans. ASME* 100: 256–262.

18. Burmeister, T., ed. 1958. *Mechanical Engineer's Handbook*. McGraw-Hill, New York, N.Y.

19. Touloukian, Y. S., ed. 1967. *Thermophysical Properties of High Temperature Solid Material*. Thermophysical Properties Research Center, Purdue Univ., Macmillian, New York.

20. *Metals Handbook*, vol. 2, 9th ed. 1978. American Society of Metals, Metals Park, Ohio.

21. Tekriwal, P., Stitt, M., and Mazumder, J. 1987. Finite element modeling of heat transfer for gas tungsten arc welding. *Metal Construction*: 599R–606R.

22. Leung, C. K., Pick, R. J., and Mok, D. H. B. 1990. Finite element modeling of a single pass weld. *WRC Bulletin* 356: 1–10.

23. Tekriwal, P., and Mazumder, J. 1988. Finite element analysis of three-dimensional transient heat transfer in GMA welding. *Welding Journal* 67(7): 150-s to 156-s.

24. Newman, S. Z. 1986. *FEM Model of 3-D Transient Temperature and Stress Fields in Welded Plates*. Ph.D. diss., Carnegie-Mellon University, Pittsburgh, Pa.

25. Engel, S. L. 1976. Kilowatt welding with a laser. *Laser Focuses*: 44–53.

26. Stern, G. 1990. Absorptivity of CW CO_2, CO and YAG-laser beam by different metal alloys. *Proc. ECLAT '90 Conf.*, pp. 25–35.

27. Kim, T. H., Chong, K. C., Yoo, B. Y., Lee, J. S., and Hwang, K. H. 1992. Absorptance of CO_2 laser beam on stainless steel and carbon steel by numerical method. *Proc. LAMP '92 Conf.*, pp. 287–292.

28. Wieting, T. J., and DeRosa, J. L. 1978. Effects of surface condition on the infrared absorptivity of 304 stainless steel. *J. Appl. Phys.* 50(2): 1071–1078.

29. Kim, J. D. 1989. Prediction of the penetration depth in laser welding. *KSME Journal* 4(1): 32–39.

30. Paul, A., and DebRoy, T. 1986. Heat transfer and fluid flow in laser melted weld pools. *Proc. Int. Conf. on Trends in Welding Research*. ed. S. A. David, pp. 29–33. American Society of Metals, Metals Park, Ohio.

31. Hibbitt, Karlsson & Sorensen, Inc. 1994. *ABAQUS Theory Manual*, Version 5.4. Providence, RI.